ELSEVIER

Journal of Controlled Release 70 (2001) 125–138

journal of controlled release

www.elsevier.com/locate/jconrel

# Continuous and highly variable rate controlled release of model drugs from sphingolipid-based complex high axial ratio microstructures

Alex S. Goldstein[a], Michael H. Gelb[a], Paul Yager[b,*]

[a]*University of Washington, Departments of Chemistry and Biochemistry, Box 351700, Seattle, WA 98195-1700, USA*
[b]*University of Washington, Molecular Bioengineering Program, Department of Bioengineering, Box 352255, Seattle, WA 98195-2255, USA*

Received 3 June 2000; accepted 16 September 2000

**Abstract**

Sphingolipids have been synthesized that contain as polar headgroups, model drugs ester-linked to the primary hydroxyl group of the ceramide core. These lipids, when allowed to self assemble below their chain-melting temperatures, either as single molecular species or in combination with other sphingolipid-derived amphiphiles, are shown to form supramolecular assemblies of varying morphologies including complex high axial ratio microstructures (CHARMs). Within these microstructures, the lipid esters are highly resistant to hydrolysis as compared to the esters dispersed as solitary monomers in aqueous solution or in a matrix of fluid phosphatidylcholine vesicles. The rate of headgroup hydrolysis within CHARMs may be manipulated over a broad range (days to years) by varying the length of the amide-linked fatty acyl chain in the ceramide core or the distance between the ester and the C-1 ceramide of the core. These microstructures, which have exceptionally high surface area display of attached headgroups, may be useful for controlled release of pharmacological agents. © 2001 Published by Elsevier Science B.V.

*Keywords:* Hydrolysis; Ester; Ceramide; Supramolecular assembly; Kinetics

## 1. Introduction

A common feature of many drug delivery systems is the use of a polymer to which a drug is covalently attached by a chemically labile linker [1–5]. Such systems have several advantages over traditional bolus administration of the drug. Rupture of the labile linkages, frequently by hydrolysis, provides a means of releasing the drug to the body at a controlled rate allowing drug concentrations to remain within a useful therapeutic range without frequent dosing. Unreleased drug is protected from premature degradation by adverse steric interactions between degradative enzymes and the polymer matrix. Furthermore, such devices may also be localized near or at the site of drug action. This may eliminate unwanted side effects and reduce the overall quantity of drug administered, all of which can lead to lower cost and better patient compliance.

We have been exploring the use of complex high

*Corresponding author. Tel.: +1-206-543-6126; fax: +1-206-543-6124.

*E-mail address:* yagerp@u.washington.edu (P. Yager).

0168-3659/01/$ – see front matter 
PII: S0168-3659(00)00335-7

axial ratio microstructures (CHARMs) as a new type of inert, self-assembled supramolecular carrier for drug delivery [6–9]. These microstructures include helical, flat, or twisted ribbons, hollow tubes, and solid or cochleate cylinders with diameters ranging from 20 to 1000 nm and lengths up to 10 μm. Several two-chain, bilayer-forming surfactants have been found to form CHARMs, among them: phospholipids with two diyne-containing fatty acyl chains [10], perfluoroalkylated fatty acyl chain containing phospholipids [11], *N,N*-dialkyl-glutamine-based amphiphiles [8,9,12,13], and sphingolipid-based amphiphiles [7,14–16].

One aspect of our study of supramolecular structures for drug delivery has involved covalently attaching drug analogs to sphingolipids; the conjugates are able to noncovalently self-assemble into CHARMs. These CHARMs are composed of bilayers of amphiphiles. For example, lipid tubules made of drug-containing amphiphiles (the drug is incorporated as part of the polar headgroup) have an extremely high surface-to-volume ratio for drug display on the surfaces that line the inner and outer walls of these hollow cylindrical microstructures. We have already demonstrated that many amphiphiles composed of different combinations of a limited variety of headgroups and CHARM-forming core lipid molecules can spontaneously self assemble into CHARMs [7]. In actuality, a wide variety of other small molecules may be attached as headgroups analogs (Fig. 1). Such headgroups are not limited to esters but may include ethers, amides, sulfonates and acetals with a broad range of sizes and hydrophobicities. Furthermore, such headgroups may have chemical functionality amenable to further modification.

CHARMs could potentially have several advantages over conventional polymeric drug delivery systems, not the least of which is that they can be composed of naturally-derived constituents, may be injected through a syringe needle into biological sites, instead of being surgically implanted and serve as localized drug depots. Although ceramide and some of the other sphingolipid metabolites are involved in cell apotopsis, the use of a sphingolipid-based drug delivery system in cancer therapy might exhibit increased efficacy as opposed to that of drug alone. Furthermore, we have demonstrated that lipid-

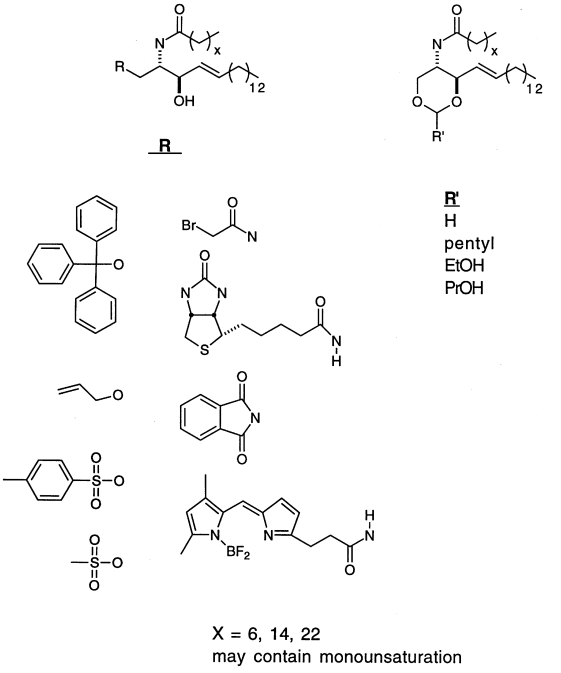


Fig. 1. Structures of compounds synthesized and studied.

based CHARMs can biodegrade very slowly and with hydrolysis kinetics that approaches desirable zero-order release for constant-rate drug delivery [6]. In another study, we demonstrated the ability of self-assembly into CHARMs to greatly reduce the rate of tryptic cleavage of a peptide that forms the polar headgroup of the CHARM-forming amphiphile [9]. In this paper we explore the potential of nonenzymatic base-catalyzed hydrolysis of esters linking the polar headgroup to the ceramide lipid core of CHARM-forming amphiphiles for controlled long term release of drugs from the microstructure. We demonstrate how the chemical structure of the amphiphile can be rationally varied to control the rate of ester hydrolysis over a broad range.

## 2. Methods and materials

### *2.1. Chemical synthesis*

$^1$H NMR spectra were obtained in $CDCl_3$, $CD_3OD$, or $D_2O$ using a Bruker 500-MHz NMR spectrometer with tetramethylsilane as an internal

standard. FAB mass spectra were obtained on a NBA matrix using a double-focusing mass spectrometer JEOL-HX110. Infrared spectra were obtained as thin films using a Perkin-Elmer 1600 Series FTIR. Silica gel (EM Science Silica Gel 60, 230–400 Mesh) was used for all flash chromatography. TLC was performed using plates coated with 250-μm Silica Gel 60 $F_{254}$ (EM Science). All reagents were used as received. Transmission electron micrographs (TEM) were obtained using a Philips EM 410 electron microscope operating at an acceleration potential of 80 kV. Samples were applied to Formvar-coated 150 mesh copper TEM sample grids and then coated with negative stain (2% aqueous ammonium molybdate, pH 5.1).

### 2.2. N-octanoyl-1-O-triphenylmethyl ceramide

*N*-Octanoyl ceramide (0.132 g, 310 μmol), triphenylmethyl chloride (0.086 g, 310 μmol) and *N*,*N*-dimethyl-4-aminopyridine (0.038 g, 310 μmol) in 50 ml toluene was refluxed overnight. The solvent was removed by rotary evaporation and the residue purified by flash chromatography (8:1–2:1 hexane:EtOAc) to provide *N*-octanoyl-1-*O*-triphenylmethyl ceramide as a white solid (0.116 g, 56%): $R_f$ (3:1 hexane:EtOAc) 0.23; IR 3303, 2923, 2851, 1728, 1646, 1077 $cm^{-1}$; $^1$H NMR 7.41–7.25 (15H), 6.06 (d, 1H, NH, $J$=8.0 Hz), 5.62 (m, 1H, C-5), 5.26 (dd, 1H, C-4, $J$=6.2, 15.5 Hz), 4.17 (m, 1H, C-2), 4.07 (dd, 1H, C-3, $J$=3.7, 8.0 Hz), 3.39 (dd, 1H, C-1, $J$=3.7, 9.9 Hz), 3.30 (39 (dd, 1H, C-1, $J$=3.7, 9.9 Hz), 2.20 (t, 2H, C-2′, $J$=7.5 Hz), 1.92 (m, 2H, C-6), 1.64 (m, 2H, C-3′), 0.88 (t, 6H, C-18, C-8′, $J$=6.8 Hz).

### 2.3. N-octanoyl-3-O-t-butyldiphenylsilyl

*N*-Octanoyl-1-*O*-triphenylmethyl ceramide (0.116 g, 174 μmol), imidazole (0.024 g, 350 μmol), and *t*-butylchlorodiphenylsilane (0.0.53 g, 190 μmol) was stirred for 19.5 h in 15 ml anhyd DMF under Ar. $Et_2O$ (30 ml) was added and the solution washed with 2×10 ml $H_2O$. The organic layer was evaporated under reduced pressure and the residue purified by flash chromatography (20:1–0:1 hexane:EtOAc and 1 ml triethylamine/100 ml of solvent) to provide impure *N*-octanoyl-1-*O*-triphenylmethyl-3-*O*-*t*-butyldiphenylsilyl ceramide as an oil. This material (0.385 g) was stirred for 3.5 h with *p*-toluenesulfonic acid monohydrate (0.036 g, 190 μmol) in 20 ml 1:1 MeOH:$CH_2Cl_2$. $Et_2O$ (20 ml) was added and the solution washed with 10 ml 5% $NaHCO_3$ (aq.). The solvent was removed by rotary evaporation and the residue purified by flash chromatography (12:1–0:1 hexane:EtOAc) to yield *N*-octanoyl-3-*O*-*t*-butyldiphenylsilyl ceramide as a white solid (0.045 g, 39%): $R_f$ (3:1 hexane:EtOAc) 0.13; IR 3374, 2923, 2851, 1636, 1554, 1113 $cm^{-1}$; $^1$H NMR 7.66–7.36 (m, 10H), 5.92 (d, 1H, NH, $J$=7.4 Hz), 5.40 (m, 2H, C-4, C-5), 4.34 (m, 1H, C-3), 3.88 (dd, 1H, C-1, $J$=4.3, 11.1 Hz), 3.84 (m, 1H, C-2), 3.61 (dd, 1H, C-1, $J$=4.3, 11.1 Hz), 1.97 (m, 2H, C-2′), 1.86 (m, 2H, C-6), 1.57 (m, 2H, C-3′), 1.07 (s, 9H, *t*-Bu), 0.88 (t, 6H, C-18, C-8′, $J$=6.1 Hz).

### 2.4. N-octanoyl-1-O-(N-acetyl-L-proline)-3-O-t-butyldiphenyl ceramide

To *N*-octanoyl-3-*O*-*t*-butyldiphenylsilyl ceramide (0.019 g, 29 μmol), *N*-acetyl-L-proline (0.013 g, 86 μmol) and *N*,*N*-dimethyl-4-aminopyridine (0.010 g, 90 μmol) in 12 ml dry 1:1 $CH_3CN$:$CH_2Cl_2$, dicyclohexylcarbodiimide (0.018 g, 86 μmol) was added and the reaction stirred overnight. The white precipitate was removed and the solvent evaporated in vacuo. Flash chromatography (5:1–0:1 hexane:EtOAc) of the residue provided *N*-octanoyl-1-*O*-(*N*-acetyl-L-proline)-3-*O*-*t*-butyldiphenylsilyl ceramide as a white solid (0.023 g, 100%): $R_f$ (3:1 hexane:EtOAc) 0.23; IR 3436, 2923, 1713, 1636, 1559 $cm^{-1}$; $^1$H NMR 7.67–7.34 (m, 10H), 6.12 (d, 1H, NH, $J$=9.3 Hz), 5.32 (dd, 1H, C-4, $J$=8.0, 15.5 Hz), 5.16 (m, 1H, C-5), 4.69 (d, 1H, a, $J$=8.0 Hz), 4.39 (m, 1H, C-3), 4.24 (bs, 2H, C-1), 4.02 (t, 1H, C-2, $J$=7.5 Hz), 3.45 (m, 2H, d), 2.16 (m, 1H, b), 2.03-1.90 (m, 7H, C-6, C-2′, b, c, NAc), 1.46 (m, 2H, C-3′), 1.06 (s, 9H, Si*t*-Bu), 0.86 (t, 6H, C-18, C-8′, $J$=7.4 Hz).

### 2.5. N-octanoyl-1-O-(N-acetyl-L-proline) ceramide

*N*-Octanoyl-1-*O*-(*N*-acetyl-L-proline)-3-*O*-*t*-butyldiphenylsilyl ceramide (0.037 g, 46 μmol) in 10 ml

anhyd THF and 50 μl 1.0 M *n*-tetrabutylammonium fluoride (in THF) was stirred for 1.5 h under Ar. The solvent was removed by rotary evaporation and the residue purified by flash chromatography (5:1–0:1 hexane:EtOAc) to provide *N*-nervonoyl-1-*O*-(*N*-acetyl-L-proline)–ceramide as a white solid (0.015 g, 58%): $R_f$ (EtOAc) 0.29; IR 3290, 2925, 2850, 1735, 1729, 1652, 1457, 1183 $cm^{-1}$; $^1H$ NMR 6.43 (d, 1H, NH, $J$=7.4 Hz), 5.73 (m, 1H, C-5), 5.47 (m, 1H, C-4), 4.46 (dd, 1H, a, $J$=3.7, 11.8 Hz), 4.39 (m, 1H, C-2), 4.34 (d, 1H, C-3, $J$=10.0 Hz), 4.09 (bs, 2H, C-1), 3.63 (m, 1H, d), 3.54 (m, 1H, d), 3.27 (bs, 1H, OH), 2.21 (m, 3H, b, C-2′), 2.09 (s, 3H, NAc), 3.01 (m, 5H, C-6, b, c, c), 1.63 (m, 2H, C-3′), 0.87 (t, 6H, C-18, C-8′, $J$=6.8 Hz).

### *2.6. N-nervonoyl-1-O-(coumarin-3-carboxylic acid) ceramide*

To *N*-nervonoyl-3-*O*-*t*-butyldiphenylsilyl ceramide (0.063 g, 71 μmol), coumarin-3-carboxylic acid (0.015 g, 78 μmol) and *N*,*N*-dimethyl-4-aminopyridine (0.010 g, 78 μmol) in 10 ml dry 1:1 $CH_3CN$:$CH_2Cl_2$, dicyclohexylcarbodiimide (0.016 g, 78 μmol) was added. The reaction was stirred for 29 h and the white precipitate was removed by filtration. The solvent was evaporated in vacuo and the residue partially purified by flash chromatography (6:1–0:1 hexane:EtOAc) to provide a mixture of starting material and *N*-nervonoyl-1-*O*-(coumarin-3-carboxylic acid)-3-*O*-*t*-butyldiphenylsilyl ceramide (0.055 g) as a clear residue. The provided analytical data is for the silylate intermediate is: $R_f$ (3:1 hexane:EtOAc) 0.31; IR 3385, 2923, 2851, 1764, 1749, 1646, 1456, 1374, 1108 $cm^{-1}$; $^1H$ NMR 7.68–7.29 (m, 15H), 5.99 (d, 1H, NH), 5.54–5.34 (m, 4H, C-4, C-5, C-15′, C-16′), 4.56 (m, 1H, C-1), 4.42 (m, 2H, C-1, C-2), 4.28 (t, 1H, C-3), 2.01–1.93 (m, 8H, C-6, C-2′, C-14′, C-17′), 1,45 (m, 2H, C-3′), 0.88 (t, 6H, C-18, C-24′).

To *N*-nervonoyl-1-*O*-(coumarin-3-carboxylic acid)-3-*O*-*t*-butyldiphenylsilyl ceramide and its starting material (0.055 g) in 20 ml dry THF, 1.0 M tetrabutylammonium fluoride (15 μl) was added. The reaction was stirred for 3.5 h, whereupon the solvent was removed by rotary evaporation and the residue purified by flash chromatography (5:1–0:1 hexane:EtOAc) to provide *N*-nervonoyl-1-*O*-(coumarin-3-carboxylic acid) ceramide as a clear residue (0.005 g, 9% from *N*-nervonoyl-3-*O*-*t*-butyldiphenylsilyl ceramide): $R_f$ (1:1 hexane:EtOAc) 0.35; IR 3508, 3282, 2923, 2851, 1785, 1718, 1660 $cm^{-1}$; $^1H$ NMR 7.72–7.65 (m, 2H), 7.41–7.37 (m, 3H), 6.58 (d, 1H, NH), 5.80 (dt, 1H, C-5), 5.53 (dd, 1H, C-4), 5.34 (t, 2H, C-15′, C-16′), 4.53 (m, 2H, C-1, C-3), 4.26 (m, 2H, C-1, C-2), 3.57 (bs, 1H, OH), 2.22 (t, 2H, C-2′), 2.02 (m, 6H, C-6, C-14′, C-17′), 1.61 (m, 2H, C-3′), 0.88 (t, 6H, C-18, C-24′).

### *2.7. N-nervonoyl-1-phthalimido-3-O-t-butyldiphenylsilyl ceramide*

To *N*-nervonoyl-3-*O*-*t*-butyldiphenylsilyl ceramide (0.111 g, 125 μmol), triphenylphosphine (0.164 g, 626 μmol), and phthalimide (0.020 g, 140 μmol) in 20 ml dry THF, diisopropylazodicarboxylate (27 μl, 140 μmol) was added. The initially orange solution was stirred for 3 h. The solvent was evaporated and the residue purified by flash chromatography (15:1–5:1 hexane:EtOAc) to provide the desired material as a white solid (0.108 g, 85%): $R_f$ (3:1 hexane:EtOAc) 0.65; IR 3436, 2923, 2851, 1733, 1539, 1021 $cm^{-1}$; $^1H$ NMR 7.81–7.34 (m, 14H), 5.62 (d, 1H, NH), 5.52 (m, 2H, C-4, C-5), 5.35 (t, 2H, C-15′, C-16′), 4.29 (m, 2H, C-2, C-3), 3.96 (dd, 2H, C-1), 1.99 (m, 8H, C-6, C-2′, C-14′, C-17′), 1.60 (m, 2H, C-3′), 1.11 (s, 9H, *t*-BuSi), 0.88 (t, 6H, C-18, C-24′).

### *2.8. N-nervonoyl-3-O-t-butyldiphenylsilyl-1-amino ceramide*

To *N*-nervonoyl-1-phthalimido-3-*O*-*t*-butyldiphenylsilyl ceramide (0.046 g, 45 μmol) in 12 ml 95% EtOH, 0.23 ml hydrazine hydrate was added. The solution was heated to reflux for 2 h. After cooling to room temperature, 15 ml of $H_2O$ and 15 ml of $Et_2O$ were added. The layers were separated and the aqueous layer was extracted with 2×15 ml $Et_2O$. The organic layers were combined and evaporated in vacuo. The residue was purified by flash chromatography (1:0–9:1 EtOAc:MeOH) to give the amine as a clear film (0.036 g, 90%): $R_f$ (MeOH) 0.48; IR 3283, 2919, 2848, 1649, 1543, 1461, 1108, 697 $cm^{-1}$; $^1H$ NMR 7.77–7.34 (m, 10H), 6.02 (d, 1H, amide), 5.34 (m, 4H, C-4, C-5, C-15′, C-16′), 4.25

(m, 1H, C-3), 3.99 (m, 1H, C-2), 3.02 (bs, 2H, C-1), 2.02–1.83 (m, 8H, C-6, C-2′, C-14′, C-17′), 1.05 (s, 9H, *t*-BuSi), 0.88 (t, 6H, C-18, C-24′ $J$=7.2 Hz).

### *2.9. N-nervonoyl-1-bromoacetamido-3-O-t-butyldiphenylsilyl ceramide*

Bromoacetic acid (0.018 g, 140 μmol) in 4 ml dry $CH_2Cl_2$ was stirred with dicyclohexylcarbodiimide (0.014 g, 68 μmol) for 20 min. The filtered solution was added to 3 ml dry DMF and the $CH_2Cl_2$ removed by rotary evaporation. The DMF solution was filtered and added to *N*-nervonoyl-3-*O*-*t*-butyldiphenylsilyl-1-amino ceramide (0.020 g, 23 μmol) in 3 ml dry DMF and stirred for 2 h. The solvent was removed under reduced pressure and the residue purified by flash chromatography (7:1–0:1 hexane:EtOAc to provide the desired material as a clear film (0.023 g, 100%): $R_f$ (1:1 hexane:EtOAc) 0.70; IR 3292, 2923, 2851, 1733, 1713, 1646, 1113, 703 $cm^{-1}$; $^1$H NMR 7.68–7.37 (m, 10H), 7.05 (bs, 1H, BrAcNH), 5.69 (d, 1H, NH, $J$=6.0 Hz), 5.49–5.38 (m, 2H, C-4, C-5), 5.35 (t, 2H, C-15′, C-16′, $J$=4.9 Hz), 4.26 (1H, C-3), 3.99 (m, 1H, C-2), 3.77 (d, 2H, BrAc, $J$=4.3 Hz), 3.48 (2H, C-1), 2.02–1.84 (m, 8H, C-6, C-2′, C-14′, C-17′), 1.44 (m, 2H, C-3′), 1.08 (s, 9H, *t*-Bu), 0.88 (t, 6H, C-18, C-24′ $J$=6.2 Hz).

### *2.10. N-nervonoyl-1-(5′-hydroxy-3-thio-pentanamido)-3-O-t-butyldiphenylsilyl ceramide*

To *N*-nervonoyl-1-bromoacetamido-3-*O*-*t*-butyldiphenylsilyl ceramide (0.012 g, 12 μmol) in 2 ml benzene, 1,8-diazabicyclo[5.4.0]undec-7-ene (1.8 μl, 12 μmol) and 2-mercaptoethanol (1.7 μl, 24 μmol) was added. The solution was stirred for 15.5 h, whereupon the solvent was removed under vacuum and the residue purified by flash chromatography (3:1–0:1 hexane:EtOAc) to provide the desired material as a clear film (0.010 g, 83%): $R_f$ (1:1 hexane:EtOAc) 0.17; IR 3323, 2923, 2851, 1651, 1615, 1313, 1241 $cm^{-1}$; $^1$H NMR 7.68–7.34 (m, 10H), 5.78 (d, 1H, NH, $J$=8.7 Hz), 5.43 (m, 2H, C-4, C-5), 5.35 (t, 2H, C-15′, C-16′, $J$=4.3 Hz), 4.23 (1H, C-3), 4.96 (m, 1H, C-2), 3.97 (t, 1H, OH), 3.72 (bs, 2H, HOC**H**$_2$), 3.45 (m, 2H, C-1), 3.18 (d, 2H, $SCH_2C(O)$, $J$=5.6 Hz), 2.78 (m, 1H, HOCC**H**$_2$S), 2.63 (m, 1H, HOCC**H**$_2$S), 2.02–1.84 (m, 8H, C-6, C-2′, C-14′, C-17′), 1.44 (m, 2H, C-3′), 1.07 (s, 9H, tBu), 0.88 (t, 6H, C-18, C-24′, $J$=6.2 Hz).

### *2.11. N-nervonoyl-1-(5′-(N-acetyl-L-proline)-3-thio-pentanamido)-3-O-t-butyldiphenylsilyl ceramide*

To *N*-nervonoyl-1-(5′-hydroxy-3-thio-pentanamido)-3-*O*-*t*-butyldiphenylsilyl ceramide (0.010 g, 10 μmol), *N*,*N*-dimethyl-4-aminopyridine (0.002 g, 20 μmol) and *N*-acetyl-L-proline (0.003 g, 20 μmol) in 5 ml dry 1:1 $CH_3CN$:$CH_2Cl_2$, dicyclohexylcarbodiimide (0.004 g, 20 μmol) was added. The solution was stirred overnight, whereupon the solvent was removed under vacuum and the residue purified by flash chromatography (3:1–0:1 hexane:EtOAc) to provide the desired material as a clear film (0.011 g, 100%): $R_f$ (EtOAc) 0.33; IR 2923, 2851, 1733, 1718, 1616, 1113 $cm^{-1}$; $^1$H NMR 7.68–7.34 (m, 10H), 5.98 (d, 1H, NH), 5.43 (m, 2H, C-4, C-5), 5.35 (t, 2H, C-15′, C-16′), 4.72 (m, 1H, α), 4.42 (m, 1H, C-2), 4.20 (m, 1H, C-3), 3.71 (m, 4H, C(O)OC**H**$_2$CS, δ), 3.49 (m, 2H, C-1), 3.18 (d, 2H, $SCH_2C(O)$, $J$=5.6 Hz), 2.78 (m, 2H, OCC**H**$_2$S), 2.20–1.91 (m, 15H, NAc, β, γ, C-6, C-2′, C-14′, C-17′), 1.08 (s, 9H, tBu), 0.88 (t, 6H, C-18, C-24′).

### *2.12. N-nervonoyl-1-(5′-(N-acetyl-L-proline)-3-thio-pentanamido) ceramide*

To *N*-nervonoyl-1-(5′-(*N*-acetyl-L-proline)-3-thio-pentanamido)-3-*O*-*t*-butyldiphenylsilyl ceramide (0.026 g, 23 μmol) in 7 ml THF, 1.0 M tetra-*n*-butylammonium fluoride in THF (23 μl, 23 μmol) was added. The solution was stirred overnight, whereupon the solvent was removed under vacuum and the residue purified by flash chromatography (1:1:0–0:1:0–0:9:1 hexane:EtOAc:MeOH) to provide the desired material as a white film (0.016 g, 76%): $R_f$ (5:1 $CHCl_3$:MeOH) 0.34; IR 3270, 2916, 2849, 1728, 1716, 1634 $cm^{-1}$; $^1$H NMR 7.83 (t, 1H, NH (C-1), 6.76 (d, 1H, NH), 5.79 (m, 1H, C-5), 5.52 (dd, 1H, C-4, $J$=4.9, 14.8 Hz), 4.51 (m, 1H, α), 4.32 (m, 1H, C-3), 4.12 (m, 1H, C-2), 3.74 (m, 2H, C(O)OC**H**$_2$CS), 3.67 (m, 1H, OCC**H**$_2$S), 3.60 (m, 3H, OCC**H**$_2$S, δ), 3.47 (m, 2H, C-1), 3.31 (bs, 2H, $SCH_2C(O)$), 2.20–1.91 (m, 15H, NAc, β, γ, C-6,

C-2′, C-14′, C-17′), 0.88 (t, 6H, C-18, C-24′); FABMS 904.4 (10%, $M^+$), 886.4 (16%, M-$H_2O$), 747.3 (10%, M–$H_2O$–AcPro).

## 3. Hydrolysis studies

### 3.1. Vesicles

Known quantities of lipids (AcPro–$C_8$–Cer, AcPro–$C_{24:1}$–Cer, Cou–$C_{24:1}$–Cer, AcPro$OCH_2$-$CH_2SCH_2CONH$–$C_{24:1}$–Cer) were dissolved in $CHCl_3$ and mixed with OPPC (Avanti Polar Lipids) so that the hydrolyzable lipid was present at 10 mol% (In general, at least 2.4 μmol of hydrolyzable lipid was present). The intimately mixed lipids were dried under vacuum for at least 30 min and then placed in aqueous 100 mM $Na_2HPO_4$, pH 9.2 so that the hydrolyzable lipid concentration was at 1.3 mM. This mixture was vortexed and sonicated in a bath device (Laboratory Supplies) at room temperature until the milky white solution became semitransparent. The vesicles were incubated at 37°C, and at various time intervals the solution was vortexed and an aliquot immediately removed. In general, the removed aliquot contained at least 0.4 μmol of ceramide. After ~25 min all solutions turned milky white. The removed aliquot was extracted four times with 1 ml $CHCl_3$ and the combined organic layers were dried under vacuum. The lipid ratios (conjugate and its corresponding ceramide hydrolysis product) were determined by $^1$H NMR in $CDCl_3$. For proline-containing lipids, the ratios of the integrands of the proline-conjugate α-hydrogen ($\delta$ 4.5) versus that of the average of C-5 and C-4 ($\delta$ 5.8, 5.4) were compared to determine the extent of hydrolysis. For coumarin-containing lipids, the ratio of the intergrands of the amides were compared (Cou–C24:1–Cer NH, $\delta$ 6.7, 24:1–Cer NH $\delta$ 6.5).

### 3.2. Formation and hydrolysis of CHARMs

CHARMs containing hydrolyzable lipid were cast from intimately mixed 1 mM DMF solutions by the addition (<20 s) of water (35% by volume). In general, the formed microstructures contained at least 2.6 μmol of hydrolyzable lipid. Organic solvent was removed by thrice pelleting the CHARMs (10°C, 10 min, 20 000×$g$), removing the supernatant and adding distilled water (equal volume to that used to precipitate CHARMs). The pooled and dried supernatants were dissolved in $CD_3OD$ and quantified by $^1$H NMR. Total lipid present in the supernatants was determined by comparing the ratio of the integrands of the terminal methyls ($\delta$ 0.8) to those of an injected internal DMF standard ($\delta$ 2.9, 2.7). The ratio of proline-conjugates to NFA–GalCer in the supernatant was determined by comparing the ratio of the integrands of the proline–lipid α-hydrogen ($\delta$ 4.5) to that of the average of C-5 and C-4 ($\delta$ 5.8, 5.4). For coumarin-conjugates:NFA–GalCer mixtures, the lipid ratio was determined by comparing the ratio of the intergrands of coumarin aromatic proton signals (2H, $\delta$ 7.8 and 2H $\delta$ 7.4) to that of the terminal methyls (6H, $\delta$ 0.8). In all cases, the lipid ratio in the pellet was identical to that of the initial DMF solution.

The assemblies, containing 1.3 mM lipid-ester conjugates, were incubated at 37°C in aqueous 100 mM $Na_2HPO_4$, pH 9.2. At various times, the assemblies were pelleted (10°C, 10 min, 20 000×$g$) and the buffer replaced. The removed supernatant was dried under vacuum and examined by $^1$H NMR ($D_2O$) to determine the proline or coumarin content. Since the lipids are virtually insoluble in water, the supernatant contained only salts and released headgroups. The NMR integrands of the acetate ($\delta$ 2.1) versus the average of an injected internal DMF standard ($\delta$ 2.9, 2.7) were compared in order to determine the quantity of released AcPro. One half the average of the integrands of coumarin peaks (2H $\delta$ 7.8 and 2H $\delta$ 7.5) versus that of an injected DMF standard (1H, $\delta$ 8.0) were compared in order to determine the quantity of released coumarin. The detection limit was determined to be ~0.1 μmol.

In order to determine the hydrolysis rate of AcPro–$C_8$–Cer as aqueous solitary monomer, AcPro–$C_8$–Cer:NFA–GalCer (1:3) CHARMs were prepared as described above. Hydrolysis was initiated, but after 4 h, the supernatant was removed as previously described and incubated at 37°C. At various times, a portion of the supernatant was removed, immediately extracted with 3×8 ml $CHCl_3$, and dried under vacuum. The ratio of ester–lipid conjugate to its hydrolyzed product was determined by $^1$H NMR ($CDCl_3$).

## 4. Amphiphile synthesis

The amphiphiles prepared in this study were composed of a ceramide lipid core and a polar headgroup attached via an ester linkage to the ceramide primary hydroxyl group (Fig. 2). Two polar headgroups, *N*-acetyl-L-proline (AcPro) and coumarin-3-carboxylic acid (Cou), served as model drugs for controlled release studies. AcPro–$C_8$–Cer and AcPro–$C_{24:1}$–Cer contain the ester linked AcPro headgroup and the *N*-linked *N*-octanoyl and *N*-nervonoyl fatty acyl chain, respectively, in the ceramide core. The synthesis of the AcPro–$C_{24:1}$–Cer material has been described previously [7] and those of AcPro–$C_8$–Cer and Cou–$C_{24:1}$–Cer are similar. In short, the primary alcohol of *N*-octanoyl or *N*-nervonoyl ceramide was protected as the triphenylmethyl ether and the secondary alcohol converted to the *t*-butyldiphenylsilyl ether. Treatment with *p*-toluenesulfonic acid revealed the primary alcohol. Carbodiimide-mediated coupling of this intermediate with the appropriate headgroup followed by fluoride treatment provided AcPro–$C_8$–Cer, AcPro–$C_{24:1}$–Cer, and Cou–$C_{24:1}$–Cer amphiphiles.

To prepare AcPro$OCH_2CH_2SCH_2CONH$–$C_{24:1}$–Cer, a ceramide analog containing an amino group in place of the primary hydroxyl and a hydrophilic tether was prepared. First, a Mitsunobu reaction of silyl-protected ceramide with phthalimide followed by hydrazine treatment generated the amine. This amine was converted to the bromoacetamide [17] and the intermediate reacted with 2-mercaptoethanol [18] to append the tether. The resultant alcohol was coupled to *N*-acetyl-L-proline, and after desilyation the desired amphiphile was obtained.

## 5. Hydrolysis of amphiphiles in vesicles

Our working hypothesis was that CHARMs composed of self-assembled lipid–drug conjugates could

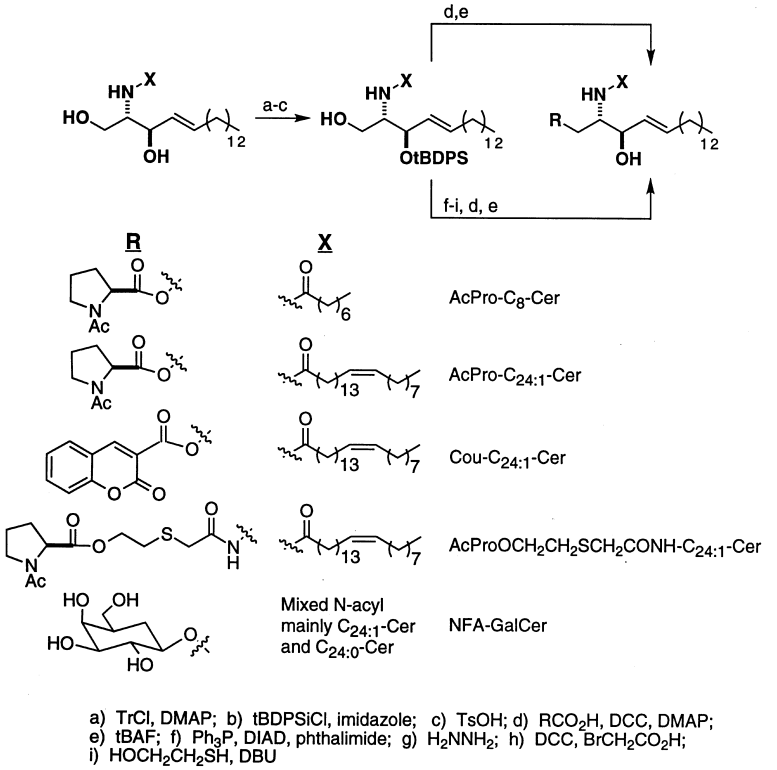


Fig. 2. Lipid synthesis.

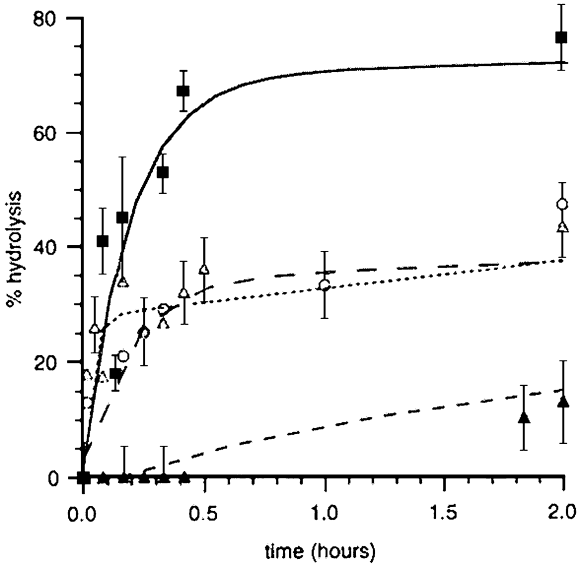


Fig. 3. Reaction progress curves for the hydrolysis of amphiphiles (1.3 mM, 10 mol%) in OPPC vesicles suspended in 100 mM phosphate, pH 9.2, 37°C. AcPro–$C_{24:1}$–Cer (---○---). Cou–$C_{24:1}$–Cer (-- --▲-- --). AcPro–$C_8$–Cer (⋯△⋯). $AcProOCH_2CH_2SCH_2CONH–C_{24:1}$–Cer (– ■ –).

release drug by spontaneous hydrolysis of the ester linking drug to 'core lipid' and that the rate of hydrolysis would be controlled over a broad range by rational manipulation of the amphiphile structure. Most of the ceramide-derived conjugates prepared in this study proved to have vanishingly low solubility as solitary monomers in the aqueous phase. Thus, we obtained hydrolysis rates for model drug–ceramide conjugates present either as CHARMs or as dilute dispersions in the bilayer surfaces of small unilamellar vesicles of 1-oleoyl-2-palmitoyl-*sn*-glycero-3-phosphocholine (OPPC). The concentration of OPPC was 13 mM, which ensured that all ceramide-based amphiphiles would be fully partitioned into vesicles; the most soluble amphiphile, AcPro–$C_8$–Cer, proved to have a solubility limit of 4±1 μM as measured using a dye inclusion method [19]. Hydrolysis kinetics were measured at 37°C in aqueous 100 mM $Na_2HPO_4$, pH 9.2 and were found to be independent of buffer concentration. The alkaline conditions, which accelerate this base-catalyzed reaction, were found to be necessary to complete the experiments within a reasonable time frame.

Fig. 3 shows the initial hydrolysis progress curves for the conjugates dispersed at 10 mol% in OPPC vesicles. Although ester hydrolysis goes to completion for all compounds over a few days, the reaction mixtures become turbid after tens of minutes, and thus, the hydrolysis half-lives were estimated from the initial velocities during the first 15–20 min (Table 1). AcPro–$C_8$–Cer and $AcProOCH_2CH_2SCH_2CONH–C_{24:1}$–Cer are hydrolyzed faster than AcPro–$C_{24:1}$–Cer. The 3-fold faster hydrolysis rate of AcPro–$C_8$–Cer may be due to the amphiphile's hydrocarbon chains not penetrating as far into the hydrophobic core of the bilayer, thus, increasing the exposure of the ester to hydroxide in the aqueous phase. Increasing the distance between the ester and the hydrophobic ceramide core is expected to lead to an increase in hydrolysis rate. Indeed, $AcProOCH_2CH_2SCH_2CONH–C_{24:1}$–Cer is hydrolyzed 3-fold faster in OPPC vesicles than is AcPro–$C_{24:1}$–Cer.

Table 1
Kinetics of amphiphile hydrolysis at pH 9.2, 37°C

| Amphiphile | OPPC Vesicles | | CHARMs | |
|---|---|---|---|---|
| | Hydrolysis half-life (h) | Rate constant $(h^{-1})\times10^{-4}$ | Hydrolysis half-life (h) | Rate constant $(h^{-1})\times10^{-9}$ |
| AcPro–$C_8$–Cer[a] | 0.14±0.02 | 8.00±1.20 | – | – |
| AcPro–$C_8$–Cer[b] | 0.17±0.03 | 6.59±0.99 | 170±20 | 64.62±0.97 |
| AcPro–$C_{24:1}$–Cer[b] | 0.53±0.08 | 2.06±0.31 | 16 300±2400 | 0.67±0.10 |
| $AcProOCH_2CH_2SCH_2CONH–C_{24:1}$–Cer[b] | 0.17±0.03 | 6.59±0.99 | 7700±1150 | 1.43±0.21 |
| Cou–$C_{24:1}$–Cer | 4.60±0.69 | 0.24±0.04 | 9100±1400 | 1.21±0.18 |
| Cou–$C_{24:1}$–Cer[c] | – | – | 9200±1400 | 1.19±0.18 |

[a] Solitary monomer.
[b] CHARMs are composed of amphiphile:NFA–GalCer (1:3).
[c] CHARMs are composed of amphiphile:NFA–GalCer (1:1).

The 9-fold slower rate of Cou–$C_{24:1}$–Cer when compared to AcPro–$C_{24:1}$–Cer is probably due to the stabilization of the ester carbonyl by the conjugated alkene of the 'prodrug'. It will be seen that these differences are negligible when ester hydrolysis is carried out in CHARMs.

Furthermore, it was determined that ester embedded in vesicles is not significantly more protected from hydrolysis than ester existing as solitary monomers. The half-life of AcPro–$C_8$–Cer, the most soluble ester studied, in the form of solitary monomers in aqueous solution was found to be 0.14 $h^{-1}$ (not shown), which is very close to the approximate half-life of 0.17 $h^{-1}$ for this compound in OPPC vesicles. These results show that the observed hydrolysis rates measured in the presence of OPPC vesicles is for the vesicle-bound amphiphile (i.e. the rate is not due to desorption of amphiphile into the aqueous phase followed by fast hydrolysis in solution) and that insertion of amphiphile into the vesicle interface does not protect the ester from base hydrolysis.

## 6. Formation and hydrolysis of CHARMs

In our previous studies, we found that the fraction of bovine brain galactocerebrosides that contain fatty acid chains lacking an α-hydroxy group (NFA–GalCer) forms hollow tubular CHARMs when precipitated from DMF by the addition of water [7]. Attempts to form CHARMs by similarly precipitating AcPro–$C_{24:1}$–Cer failed in that amorphous aggregates were consistently observed by optical and transmission electron microscopy (not shown). We found that co-dispersions of NFA–GalCer with up to 25% AcPro–$C_{24:1}$–Cer gave CHARMs similar to those formed from pure NFA–GalCer [7]. On the other hand, the amphiphile Cou–$C_{24:1}$–Cer forms tubular CHARMs when precipitated from DMF in the presence and absence of NFA–GalCer (Fig. 4A, B). However, CHARMs formed from pure Cou–$C_{24:1}$–Cer typically had 5-fold larger diameters and appeared more irregularly shaped than CHARMs formed with NFA–GalCer (Fig. 4A, B). Cou–$C_{24:1}$–Cer:NFA–GalCer CHARMs have similar morphology to those formed from pure NFA–GalCer and from AcPro:NFA–GalCer. These CHARMs are typically 20 nm in diameter with lengths up to micrometers. The transmission electron image (Fig. 4A) shows negative stain within the lumen of the tubular CHARMs. These CHARMs tend to cluster in groups of two or more. Similarly shaped CHARMs are formed when the headgroup-extended amphiphile AcPro$OCH_2CH_2SCH_2CONH$–$C_{24:1}$–Cer is co-dispersed in NFA–GalCer (not shown). Other methods for CHARM preparation from these ceramide-derived amphiphiles have been described previously [7]; the DMF/water precipitation method is preferred because of its simplicity and reproducibility in generating CHARMs with consistent morphology.

The hydrolytic release of AcPro and Cou from CHARMs was studied under the same conditions as those used for the amphiphiles embedded in OPPC vesicles. As in the case of vesicles, hydrolysis progress curves were monitored by using $^1$H-NMR to quantify the amount of released headgroup in the supernatant after CHARMs were pelleted by centrifugation. Hydrolysis progress curves are shown in Fig. 5, and it is clear that the amphiphile half-lives are significantly greater than those measured with OPPC as the host lipid (Table 1). The rank order of increasing half-life is AcPro–$C_8$–Cer: NFA–GalCer (1 : 3) < AcPro$OCH_2CH_2SCH_2CONH$ – $C_{24:1}$ – Cer : NFA–GalCer (1:3)<AcPro–C24:1–Cer:NFA–GalCer (1:3)<Cou–$C_{24:1}$–Cer:NFA–GalCer (1:1)≈ Cou–$C_{24:1}$–Cer (Table 1). The hydrolysis half-lives at pH 9.2 varied over a large range, from seven to ≈680 days. The material was hydrolyzed in screw top containers that prevented evaporation. The pH values of harvested supernatants were identical to those of the initial buffer. Finally, there is no evidence that bacteria or mold grew during the course of the experiment. Such opportunistic organisms probably would not let hydrolyzed material such as proline go unsequestered, especially in such a poor growth media.

The amphiphile AcPro–$C_8$–Cer reacts 1000-fold slower when co-dispersed with NFA–GalCer (hydrolytically inert under these conditions) in CHARMs than when present in OPPC vesicles, whereas the slowest hydrolyzing amphiphile AcPro–$C_{24:1}$–Cer is broken down 30 700-fold slower when present in CHARMs than in OPPC vesicles. Cou–$C_{24:1}$–Cer and AcPro–$C_{24:1}$–Cer are hydrolyzed in CHARMs at similar rates (only 1.8-fold difference). Compari-

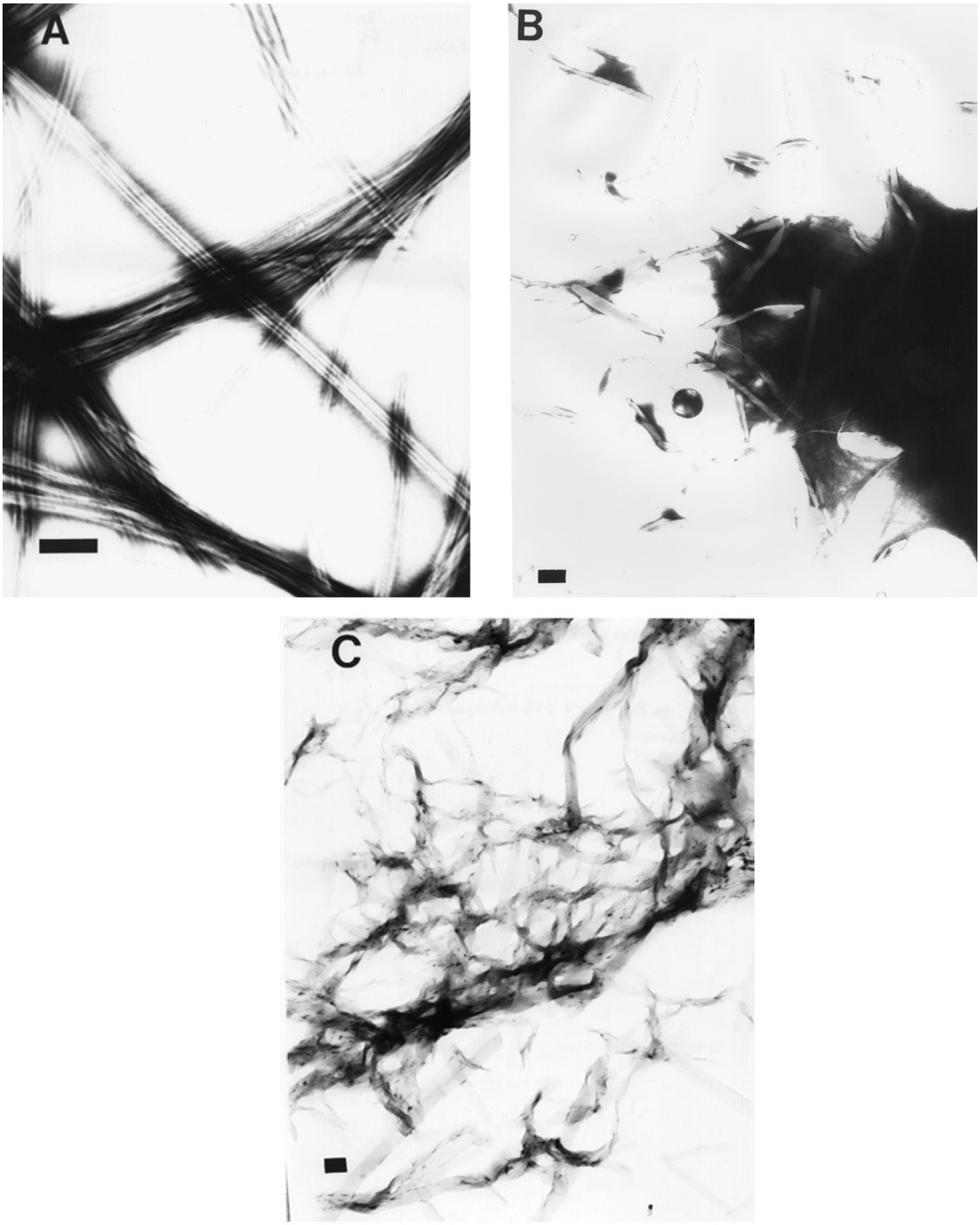


Fig. 4. Negatively stained transmission electron micrographs: (A) Cou–$C_{24:1}$–Cer:NFA–GalCer (1:1). Scale bar 200 nm. This image is representative of all NFA–GalCer containing CHARMs prior to hydrolysis; (B) Pure Cou–$C_{24:1}$–Cer CHARMs. Scale bar 500 nm; (C) AcPro–$C_8$–Cer:NFA–GalCer (1:3) CHARMs during and after hydrolysis. Scale bar 200 nm.

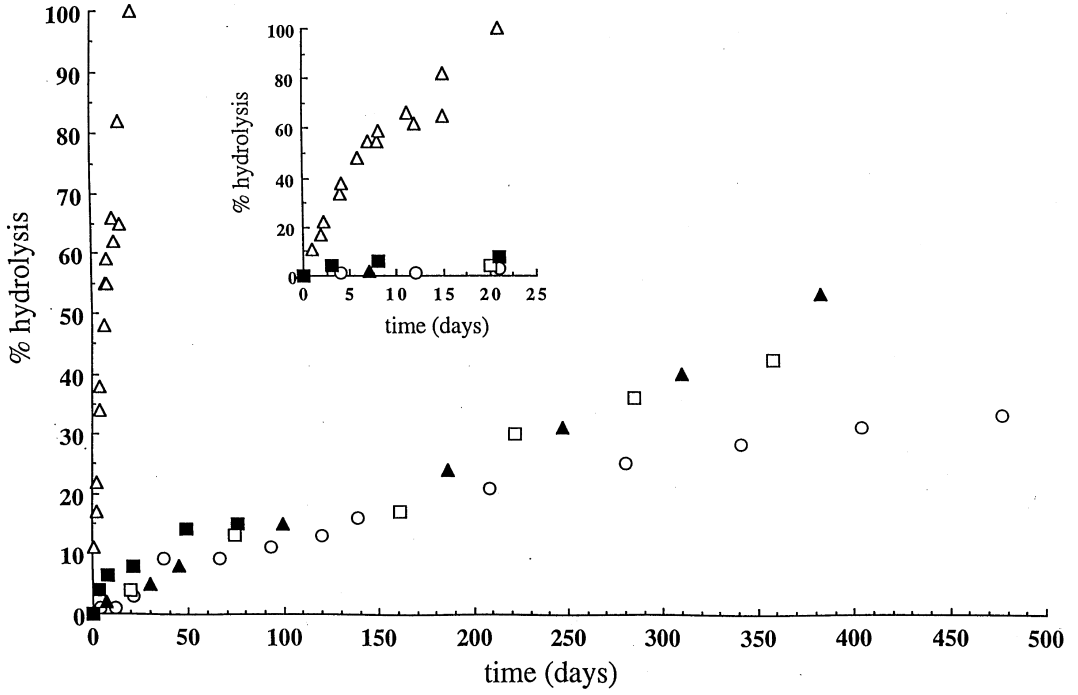


Fig. 5. Reaction progress curves for the hydrolysis of CHARM-embedded amphiphiles (1.3 mM) in 100 mM phosphate, pH 9.2, 37°C. (---○---) AcPro–$C_{24:1}$–Cer:NFA–GalCer (1:3). (-- --▲-- --) Cou–$C_{24:1}$–Cer. (--·--□--·--) Cou–$C_{24:1}$–Cer:NFA–GalCer (1:1). (···△···) AcPro–$C_8$–Cer:NFA–GalCer (1:3). (– ■ –) AcPro$OCH_2CH_2SCH_2CONH$–$C_{24:1}$–Cer:NFA–GalCer (1:3). ] NFA–GalCer is not hydrolyzed under these conditions.

son of assemblies containing pure Cou–$C_{24:1}$–Cer and mixed lipid assemblies composed of Cou–$C_{24:1}$–Cer and NFA–GalCer (1:1 mole ratio) show identical half-lives implying that NFA–GalCer does not perturb the hydrolysis. Finally, AcPro$OCH_2CH_2SCH_2CONH$–$C_{24:1}$–Cer present in NFA–GalCer CHARMs is hydrolyzed ~2-fold more rapidly than AcPro–$C_{24:1}$–Cer also present in NFA–GalCer CHARMs (and 45 300-fold slower than when present in vesicles). In this case the ester linkage of AcPro$OCH_2CH_2SCH_2CONH$–$C_{24:1}$–Cer is presumably protruding into the aqueous phase further away from the interfacial region than in the case of AcPro–$C_{24:1}$–Cer containing CHARMs.

We postulate that the marked retardation of ester hydrolysis in CHARMs is due to tight crystalline packing of the amphiphile headgroup with neighboring amphiphiles. Either hydroxide is unable to approach the ester linkage or steric constraints prevent the formation of the requisite tetrahedral intermediate. Based on modeling studies, the ester of AcPro$OCH_2CH_2SCH_2CONH$–$C_{24:1}$–Cer is roughly 3.5 Å above the NFA–GalCer van der Waals surface (Fig. 6). However, for the other amphiphiles, which do not have the headgroup extension, the ester group is buried about 0.5 Å below the NFA–GalCer van der Waals surface. This model is based on the crystal structure of a NFA–GalCer derivative in which the alkyl chains are highly shortened [20–22]. Furthermore, more recent studies using NMR and molecular modeling indicate that the GalCer crystal structure is similar to the solution state conformation [22–27]. Lipid in which AcPro, Cou and the chain-extended headgroups replace the galactose of the chain-shortened host lipid were energy minimized using CS Chem3D Pro. These ester monomer structures were then inserted into a lipid lattice so that the bis-alkyl hydrophobic chains were indistinguishable from the host lipid. Visual inspection of the model showed no violations of van der Waals radii. Further energy minimization of the entire lattice did not significantly alter the gross lipid conformation. Such modeling

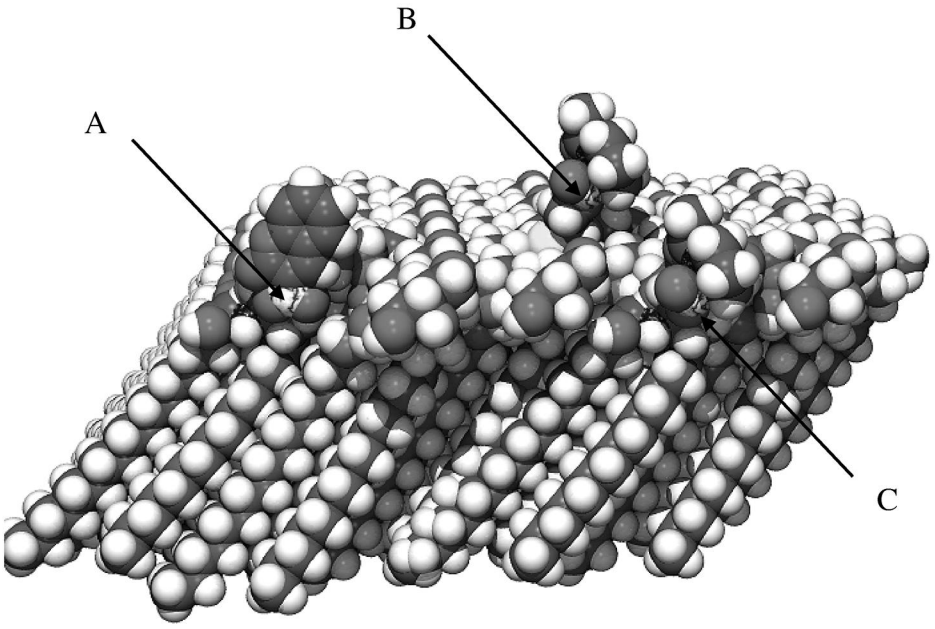


Fig. 6. Model ester headgroups imbedded in NFA–GalCer matrix. Arrow points to the carbonyl carbon of hydrolyzable ester: (A) Coumarin; (B) AcProOCH$_2$CH$_2$SCH$_2$CONH–C$_{24:1}$–Cer; (C) AcPro.

studies support the idea that crystalline packing of amphiphiles in CHARMs is the basis for protection from alkaline hydrolysis.

Two mechanisms for hydrolysis of the ester linkage in ceramide-derived amphiphiles were considered. In mechanism (1), the slow rate of hydrolysis is due to attack of hydroxide onto the ester carbonyl of the amphiphile present in CHARMs. In mechanism (2), amphiphile present in the aqueous phase but not CHARM-embedded amphiphile undergoes hydrolysis. Based on the following arguments, it seems clear that mechanism (1) is operative. The half-time for hydrolysis of AcPro–C$_8$–Cer present as solitary monomers in the aqueous phase is 0.14 h (first-order rate constant of $7.85\times10^{-5}$ h$^{-1}$). It is difficult to measure the rate of hydrolysis of AcPro–C$_{24:1}$–Cer in the form of solitary monomers because of the exceedingly low solubility of this compound. However, it is reasonable to assume that this longer-chain amphiphile in the aqueous phase will hydrolyze at a rate similar to that of AcPro–C$_8$–Cer in the aqueous phase. Thus, according to mechanism (2), the rate of hydrolysis of AcPro–C$_{24:1}$–Cer in CHARMs should be equal to the concentration of amphiphile in the aqueous phase that is in equilibrium with amphiphile in CHARMs multiplied by the rate constant for hydrolysis of solitary monomeric AcPro–C$_{24:1}$–Cer. This calculation gives an aqueous phase concentration of AcPro–C$_{24:1}$–Cer in the presence of 5.2 mM CHARM lipid of 0.6 μM. This concentration is certainly much higher than any reasonable estimate of the aqueous phase concentration of AcPro–C$_{24:1}$–Cer, based on the fact that the upper limit for the solubility of GalCer with a 24:0 fatty acyl chain is 0.1 nM [28]. Thus, it seems clear that mechanism (2) is ruled out and that it is the CHARM-embedded AcPro–C$_{24:1}$–Cer that is undergoing hydrolysis [mechanism (1)]. In addition, we found that the half-life for hydrolysis of AcPro–C$_8$–Cer is independent of its mole fraction in NFA–GalCer CHARMs (in the range 0.10–0.25) under conditions in which total lipid concentration is held constant (not shown). Since the aqueous phase concentration of AcPro–C$_8$–Cer drops as the amount of NFA–GalCer is increased, the half-time of hydrolysis should have increased if aqueous phase

amphiphile is being hydrolyzed. Similar arguments apply to amphiphiles with the coumarin headgroup and with the chain-extended AcPro.

Given that CHARM-embedded amphiphile is being hydrolyzed, the possibility remains that there exist transient fluid domains in the microstructure, and amphiphile present in these domains is being hydrolyzed in preference to material located in crystalline domains. This possibility seems unlikely based on the fact that differential scanning calorimetry of mixed CHARMs composed of NFA–GalCer together with AcPro–$C_8$–Cer, AcPro–$C_{24:1}$–Cer, or Cou–$C_{24:1}$–Cer showed crystalline-to-liquid order–disorder transitions well above 37°C (57–70°C, not shown). This suggests that the mixed lipid CHARMs are entirely crystalline.

Tubules composed of AcPro–$C_8$–Cer:NFA–GalCer (1:3) were examined for morphological changes as hydrolysis progressed (Fig. 4C). After 48 h (first examination), the tubular microstructures have been replaced by ribbon-like structures that persist even upon completion of hydrolysis. This final morphology is dissimilar to that seen for microstructures made from the hydrolysis product [*N*-octanoyl–ceramide:NFA–GalCer (1:3)]. This latter mixture gives 20-nm diameter tubules when a DMF solution is mixed with water (not shown).

## 7. Conclusion

We have demonstrated that the self assembly of sphingolipid derivatives with ester linked headgroups into CHARMs results in greatly enhanced resistance to alkaline hydrolysis. Such lipids may form CHARMs independently or as mixtures of surfactants. The overall rate of hydrolysis is dependent on the ester–lipid embedded in the CHARM. Different headgroup esters can be used and the hydrolysis rate manipulated by three orders of magnitude by varying the number of carbons in the *N*-linked fatty acyl chain or by changing the position of the cleavable ester moiety in relationship to the hydrophobic ceramide core. This adjustable kinetics has promise for allowing controlled release of bioactive molecules from the microstructures in vivo and in vitro and may also allow for the simultaneous delivery of multiple drugs.

## Acknowledgements

The authors thank Dr. Anatoly Lukyanov for DSC information and Dr. Paul Carlson for TEM, molecular modeling and generation of Fig. 6. This work was supported by a grant from the Whitaker Foundation.

## References

[1] A.K. Dash, G.C. Cudworth 2nd, Therapeutic applications of implantable drug delivery systems, J. Pharmacol. Toxicol. Methods 40 (1998) 1–12.
[2] R. Jain, N.H. Shah, A.W. Malick, C.T. Rhodes, Controlled drug delivery by biodegradable poly(ester) devices: different preparative approaches, Drug Dev. Ind. Pharm. 24 (1998) 703–727.
[3] V.R. Sinha, L. Khosla, Bioabsorbable polymers for implantable therapeutic systems, Drug Dev. Ind. Pharm. 24 (1998) 1129–1138.
[4] J.M. Harris, S. Zalipsky (Eds.), Poly(ethylene glycol), ACS Symposium Series, Vol. 680, American Chemical Society, San Francisco, 1997.
[5] H. Noguchi, H. Iwata, Y. Ikada, Synthesis of monomeric and polymeric conjugates carrying a thrombin inhibitor through an ester bond, J. Biomed. Mater. Res. 39 (1998) 621–629.
[6] P.A. Carlson, M.H. Gelb, P. Yager, Zero-order interfacial enzymatic degradation of phospholipid tubules, Biophys. J. 73 (1997) 230–238.
[7] A.S. Goldstein, A.N. Lukyanov, P.A. Carlson, P. Yager, M.H. Gelb, Formation of high-axial-ratio-microstructures from natural and synthetic sphingolipids, Chem. Phys. Lipids 88 (1997) 21–36.
[8] K.C. Lee, A.N. Lukyanov, M.H. Gelb, P. Yager, Formation of high axial ratio microstructures from peptides modified with glutamic acid dialkyl amides, Biochim. Biophys. Acta 1371 (1998) 168–184.
[9] K.C. Lee, P.A. Carlson, A.S. Goldstein, P. Yager, M.H. Gelb, Protection of a decapeptide from proteolytic cleavage by lipidation and self-assembly into high-axial-ratio microstructures: A kinetic and structural study, Langmuir 15 (1999) 5500–5508.
[10] P. Yager, P.E. Schoen, Formation of tubules by a polymerizable surfactant, Mol. Cryst. Liq. Cryst. 106 (1984) 371–381.
[11] M.P. Krafft, F. Giulieri, J.G. Riess, Microtubules from fluorinated phosphorylated amphiphiles in aqueous/alcoholic and non-aqueous solvents, Phosphorous, Sulfur and Silicon 111 (1996) 708.
[12] K. Yamada, H. Ihara, T. Ide, T. Fukumoto, C. Hirayama, Formation of helical super structure from single-walled bilayers by amphiphiles with oligo-L-glutamic acid-head group, Chem. Lett. 10 (1984) 1713–1716.
[13] T. Shimizu, M. Hato, Self-assembling properties of synthetic peptidic lipids, Biochim. Biophys. Acta 1147 (1993) 50–58.
[14] D.D. Archibald, P. Yager, Microstructural polymorphism in

bovine brain galactocerebroside and its two major subfractions, Biochemistry 31 (1992) 9045–9055.
[15] D.D. Archibald, S. Mann, Structural studies of lipid fibers formed by sphingosine, Biochim. Biophys. Acta 1166 (1993) 154–162.
[16] V.S. Kulkarni, W.H. Anderson, R.E. Brown, Bilayer nanotubes and helical ribbons formed by hydrated galactosylceramides: acyl chain and headgroup effects, Biophys. J. 69 (1995) 1976–1986.
[17] F.A. Robey, R.L. Fields, Automated synthesis of *N*-bromoacetyl-modified peptides for the preparation of synthetic peptide polymers, peptide–protein conjugates, and cyclic peptides, Anal. Biochem. 177 (1989) 373–377.
[18] E. Ono, H. Miyake, T. Saito, A. Kaji, A convenient synthesis of sulfides, formaldehyde dithioacetals, and chloromethyl sulfides, Synthesis 11 (1980) 952–953.
[19] R.M. Brito, W.L. Vaz, Determination of the critical micelle concentration of surfactants using the fluorescent probe *N*-phenyl-1-naphthylamine, Anal. Biochem. 152 (1986) 250–255.
[20] I. Pascher, S. Sundell, Molecular arrangements in sphingolipids. The crystal structure of cerebroside, Chem. Phys. Lipids 20 (1977) 179–191.
[21] I. Pascher, Molecular arrangements in sphingolipids. Conformation and hydrogen bonding of ceramide and their implication on membrane stability and permeability, Biochim. Biophys. Acta 455 (1976) 433–451.
[22] I. Pascher, M. Lundmark, P.G. Nyholm, S. Sundell, Crystal structures of membrane lipids, Biochim. Biophys. Acta 1113 (1992) 339–373.
[23] P.G. Nyholm, I. Pascher, Orientation of the saccharide chains of glycolipids at the membrane surface: conformational analysis of the glucose–ceramide and the glucose–glyceride linkages using molecular mechanics (MM3), Biochemistry 32 (1993) 1225–1234.
[24] P.G. Nyholm, I. Pascher, S. Sundell, The effect of hydrogen bonds on the conformation of glycosphingolipids. Methylated and unmethylated cerebroside studied by X-ray single crystal analysis and model calculations, Chem. Phys. Lipids 52 (1990) 1–10.
[25] P.G. Nyholm, I. Pascher, Steric presentation and recognition of the saccharide chains of glycolipids at the cell surface: favoured conformations of the saccharide–lipid linkage calculated using molecular mechanics (MM3), Int. J. Biol. Macromol. 15 (1993) 43–51.
[26] H. Lofgren, I. Pascher, Molecular arrangements of sphingolipids. The monolayer behaviour of ceramides, Chem. Phys. Lipids 20 (1977) 273–284.
[27] K.S. Hamilton, H.C. Jarrell, K.M. Briere, C.W. Grant, Glycosphingolipid backbone conformation and behavior in cholesterol-containing phospholipid bilayers, Biochemistry 32 (1993) 4022–4028.
[28] J.D. Jones, P.F. Almeida, T.E. Thompson, Spontaneous interbilayer transfer of hexosylceramides between phospholipid bilayers, Biochemistry 29 (1990) 3892–3897.